Geomechanics and Engineering, *Vol. 41, No. 2 (2025) 233-241*
https://doi.org/10.12989/gae.2025.41.2.233

Applicability to engineered slopes of water repellent soils using laboratory model tests

Byeong-Su Kim*[1] and Shoji Kato[2a]

[1]*Department of Civil & Environmental Engineering, Dankook University, 152, Jukjeon-ro, Suji-gu, Yongin City, Gyeonggi-do 16890, Korea*
[2]*Graduate School of Engineering, Kobe University, Rokkodai-cho, Nada-ku, Kobe City, Hyogo 657-8501, Japan*

(*Received December 4, 2024, Revised April 5, 2025, Accepted April 9, 2025*)

Abstract. In recent years, ground disasters such as the collapse of unsaturated river levees have frequently occurred due to the seepage and erosion of rainwater during heavy rain. Applying water repellent soil to engineered slopes can be one of the solutions to prevent rainwater infiltration. For this, previous studies have verified the effects of rainfall intensity, layer thickness, and grain size distribution of geomaterials through water infiltration head (WIH) tests. In this study, to objectively verify the applicability of the impermeable layer of hydrophobic materials to field slopes, a series of laboratory embankment model tests were conducted on these three influences. Like the trend of the results of the previous WIH test, the water-shielding performance of the hydrophobic geomaterial could be determined through the results obtained from the model tests. As a result, it can be said that the application of hydrophobic geomaterials to engineered slopes could be a good alternative to maintain slope stability against rainwater infiltration.

Keywords: hydrophobic material; laboratory embankment model test; rainwater infiltration; water infiltration test

1. Introduction

Although many researchers have studied slope collapse caused by rainfall and strengthened water-impermeable and drainage functions, disasters caused by rainfall frequently occur in various regions (Doan 2023, Rajabian 2023). The results of studies based on unsaturated soil mechanics revealed that the failure mechanism of geostructures due to water infiltration is related to the reduction of shear strength with matric suction of unsaturated soils (Fredlund *et al.* 1978, Karube and Kawai 2001, Rahardjo *et al.* 2007, Sun *et al.* 2008, Kim *et al.* 2010, Oh and Vanapalli 2018, Yu *et al.* 2023). In practice, installing a water-impermeable layer or applying drainage techniques to prevent water infiltration into the ground and maintain the unsaturated state inside the ground is important for maintaining the stability of the geostructures (Heibaum 2016, Lee *et al.* 2023). Methods such as placing concrete and impermeable sheets on the surface of geostructures with a drainage system have been generally used to protect against water infiltration. Although these structural approaches were effective, they were costly and prone to problems due to maintenance and environmental considerations.

On the other hand, although geomaterials that exist in nature generally become hydrophilic (wettable condition), it is well-known that hydrophobized natural geomaterials are also widely distributed worldwide (Wallis and Horne 1992). The water repellency of natural geomaterials is mostly due to the chemical reactions of organic pollutants generated by the corrosion of plants, natural disasters such as forest fires, and environmental pollution such as oil spillages (Debano and Krammes 1966, Ritsema *et al.* 1998, Jaramillo *et al*. 2000, Ritsema and Dekker 2000). The water repellency of the surface of natural geomaterials, which is related to the solid-liquid contact angle and the surface energy, affects infiltration, evaporation, erosion, and the hydrologic balance of the ground (Wallis and Horne 1992, Ritsema and Dekker 2000, Bauters *et al.* 2000, Doerr *et al*. 2006, Meek *et al.* 2020).

As a countermeasure against a disaster like the slope failure due to rain infiltration, installing a highly water-impermeable layer using hydrophobic (water-repellent) materials to the engineered slopes can be an effective method to prevent water infiltration into the slopes. Although there have been many studies on the surface properties of hydrophobic materials in the fields of soil science and chemical materials, the study on the applicability of impermeable ground materials in the field of geotechnical engineering was first attempted by Kim *et al*. (2021). Kim *et al*. (2021) investigated the water-shielding performance and the hydrophobicity using six hydrophobic sandy soils in terms of dry density, mean particle size, surface condition, and layer thickness through the water infiltration head (WIH) test. Based on the results obtained, they specified the minimum layer thickness for the hydrophobic ground material to have the maximum water-shielding performance. They also proposed the selection criteria for geomaterials based on the relationship

*Corresponding author, Associate Professor
E-mail: bs.kim@dankook.ac.kr
[a]Associate Professor

ISSN: 2005-307X (Print), 2092-6219 (Online)

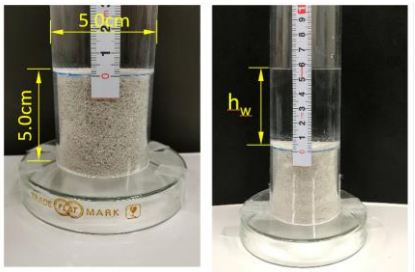

Fig. 1 Water infiltration head (WIH) test

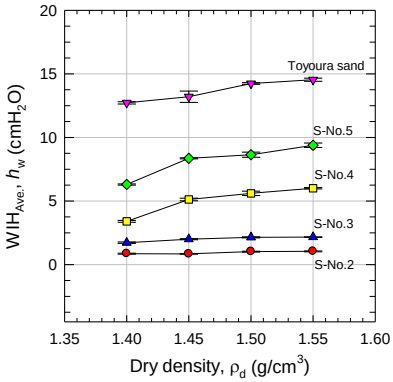

Fig. 2 Relationship between dry density and WIH (After Kim *et al*. 2021)

between the percentage of particle size less than 2 mm and WIH (i.e., water infiltration head, h_w). However, since their test results were based only on the results obtained through the WIH test, it is necessary to verify whether their research results are valid in an engineered slope.

In this study, based on the WIH test results of Kim *et al*. (2021), a series of laboratory embankment model tests are conducted for three effects: rainfall intensity, layer thickness, and particle size distribution, to evaluate the water-shielding performance of hydrophobic geomaterials and their applicability to actual engineered slopes. In Case 1, three rainfall intensities of 20, 50, and 100 mm/h are applied. In Case 2, hydrophobic Toyoura sand is used to prepare the thinnest layer thickness of 0.5 cm. In Case 3, soil samples mixed with hydrophobic Toyoura sand and Silica sand No. 2 in a ratio of 4:6 are used.

2. Literature review

2.1 What is water infiltration head test?

The water infiltration head (WIH) test measures the water head (h_w, cmH_2O) that hydrophobic materials can withstand without water infiltration as shown in Fig. 1. In the WIH test, the specimen size was 5.0 cm in diameter and 5.0 cm in height, and a transparent circular tube made of acrylic material was used. The measured value was defined as the water infiltration head and can be used as a critical indicator to determine the hydrophobicity and water-shielding performance of hydrophobic materials. Specifically, the water head at the moment when water permeates the surface of a specimen of the hydrophobic soil

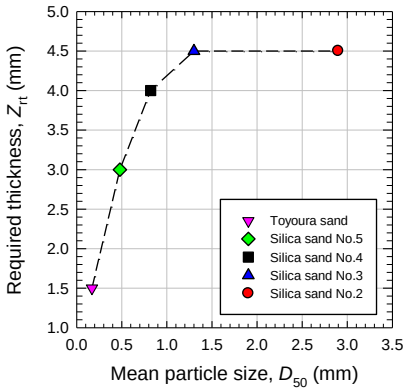

Fig. 3 Relationship between mean particle size and required thickness (After Kim *et al*. 2021)

made under predetermined conditions is the WIH value. In the WIH test, water is dripped onto the surface of a specimen made at a specified dry density in an acrylic cylinder, and the head (h_w) is increased until infiltration begins, and the head at the time of infiltration is measured. To establish criteria for applying hydrophobic geomaterials to engineered slopes, Kim *et al*. (2021) performed the WIH tests using silica sand No. 2 to No. 5 and Toyoura sand in three cases: Case 1: Dry density, Case 2: Layer thickness, and Case 3: Grain size distribution of geomaterials.

2.2 Case 1: Effect of dry density

In the study of Kim *et al*. (2021), to investigate the effect of dry density on the WIH, the dry density was changed to four values. The relationship between dry density and WIH is shown in Fig. 2. The WIH increases with increasing dry density for all samples. On the other hand, the WIH decreases with increasing average particle size for all dry densities. The change in the WIH due to differences in dry density and particle size is related to the voids between particles. It can be understood that when the dry density is large and the mean particle size is small, the voids become small, making it difficult for water to infiltrate, and thus exhibiting high water-shielding properties.

2.3 Case 2: Effect of layer thickness

In Case 2, the minimum layer thickness required to obtain sufficient WIH, that can maintain the maximum water resistance performance of hydrophobic ground materials, was examined. Determining the minimum water barrier thickness can reduce the amount of on-site impermeable material used, which will lead to reduced construction costs. For this, Silica sand Nos. 2 ~ 5 and Toyoura sand were used, and the dry density was set to ρ_d = 1.50 g/cm^3. Based on the WIH test using a test piece with a height (thickness) of 5 cm, specimens were repeatedly manufactured by decreasing the height of the specimens by 0.5 mm each, and the WIH test was performed on each specimen. The specimen height when the minimum WIH value for the layer thickness of 5.0 cm obtained in Case 1 was equal to the required layer thickness (Z_{rt}). From the

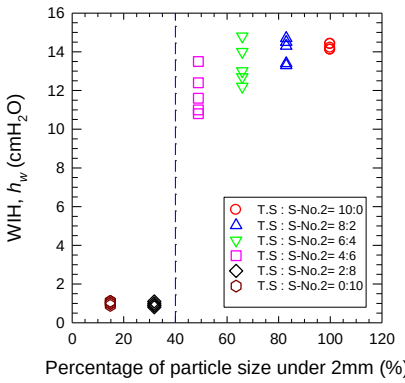

Fig. 4 Relationship between percentage of particle size less than 2 mm and WIH (After Kim *et al*. 2021)

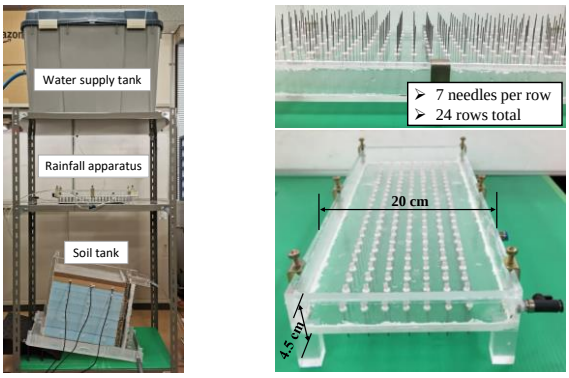

(a) Apparatus of model test (b) Rainfall apparatus

Fig. 5 Test apparatus setup for model testing

results, all samples had sufficient waterproofing properties when the layer thickness was 4.5 mm or less, as shown in Fig. 3. Therefore, these results showed that the thickness of the impermeable layer on site can be determined at 4.5 mm or more and that construction costs can be reduced.

2.4 Case 3: Effect of grain size distribution of geomaterials

In Case 3, the effect of the grain size distribution of geomaterials on water-shielding performance was examined. For this, the WIH tests were conducted with four mixing ratios (Toyoura sand: silica sand No. 2) of 2:8, 4:6, 6:4, and 8:2 by weight. Fig. 4 shows the relationship between the percentage of particle size less than 2 mm and WIH. It was found that when the curvature coefficient (C_c) is under 1.0 and the content of 2.0 mm or less is over 40%, the WIH value is significantly high. Thus, it can be said that the curvature coefficient and the content of 2.0 mm or less are important measures for determining whether a hydrophobic geomaterial exhibits excellent water-shielding performance at an actual construction site.

3. Laboratory embankment model test of hydrophobic impermeable layer materials

In this study, to examine the water-shielding performance and applicability to engineered slopes of hydrophobic geomaterials as slope-filling materials, a series of laboratory model tests were conducted for three conditions based on the conditions of the WIH test (Case 1: Effect of rainfall intensity, Case 2: Effect of layer thickness, and Case 3: Effect of the grain size distribution of geomaterials) (Kim *et al*. 2021). In Case 1, three patterns of rainfall intensity (I) (20, 50, and 100 mm/h) were applied, and in Case 2, the layer thickness of a hydrophobic layer was set to 0.5 cm. Lastly, in Case 3, a mixed hydrophobic material with a mixing ratio (hydrophobic sand: silica sand No. 2) of 4:6 was applied as the slope layer material.

3.1 Test apparatus and soil samples for model tests

Fig. 5(a) shows a model test apparatus used in the model test. The apparatus includes a water supply tank, a rainfall apparatus, and a soil tank. The inside of the soil tank was 45.5 cm long, 47.0 cm high, and 15.0 cm wide. The thickness of the acrylic material was 20 mm. Fig. 5(b) shows the rainfall apparatus, which was 500 mm long, 45 mm high, and 200 mm wide. To properly reproduce the rainfall phenomenon, 161 needles were installed at 20 mm intervals (7 needles per row, 24 rows total). Fig. 6 shows the grain size distribution curves of soil samples: Toyoura sand, Masado(i.e., weathered granite soil), Silica sand No.2, and Gravel. Table 1 summarizes the physical properties of Toyoura sand and Masado (i.e., weathered granite soil), Gravel (used as a material of drainage path), and Silica sand No. 2 used in model tests.

Table 1 Physical properties of the soil samples

Sample	Toyoura sand	Masado	Gravel	Silica sand No.2
G_s (g/cm^3)	2.64	2.58	2.65	2.64
w_L (%)	-	24.6	-	-
w_p (%)	-	N.P	-	-
$\rho_{d\,max}$ (g/cm^3)	1.64	1.88	1.67	1.57
$\rho_{d\,min}$ (g/cm^3)	1.37	-	1.45	1.39
D_{50} (cm)	1.69	0.38	4.65	2.90
F_c (%)	0	18.4	0	0
C_u	1.63	13.7	2.24	1.19
C_c	0.97	-	0.84	1.07
k_{sat} (m/s)	1.45×10^{-4}	1.40×10^{-6}	2.44×10^{-3}	2.16×10^{-3}

Note: G_s = specific gravity, w_L = liquid limit, w_p = plastic limit, $\rho_{d\,max}$ & $\rho_{d\,min}$ = maximum and minimum dry densities, D_{50} = mean particle size, F_c = passing percent under 75μm, C_u = uniformity coefficient, C_c = curvature coefficient, and k_{sat} = saturated hydraulic conductivity

3.2 Manufacturing method of hydrophobic geomaterials

In this study, a hydrophobization reaction process using triethoxysilane was applied to produce hydrophobic geomaterials. Since the surface chemical groups of silica sand and Toyoura sand are mainly interfacial siloxanes (Si–O–Si), the particle surfaces of these samples become hydrophobic due to the dehydroxylation of the surface hydroxyls in the hydrophobization reaction process using triethoxysilane (i.e., silanization process) (Vigil *et al*. 1994, Li *et al*. 2014). Here, Toyoura sand and Silica sand No. 2

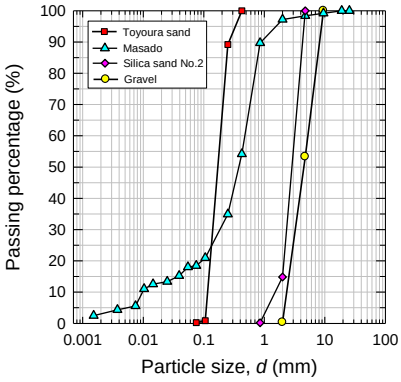

Fig. 6 Grain size distribution curves of soil samples

have silica (SiO_2) contents of 92.6% and 98.0%, respectively.

The silanization process was applied to the samples of Toyoura sand and silica sand No. 2 using a mixed chemical solution of n-octyltriethoxysilane ($C_{14}H_{32}O_3Si$) and isopropyl alcohol to stably produce hydrophobic geomaterials. A mixed chemical solution of n-octyltriethoxysilane (5 ml) and isopropyl alcohol (495 ml) was prepared for 500 g of soil sample. After the prepared soil sample was immersed in the mixed solution, the solution was then sealed and stored at room temperature (20–24°C) for 72h. In this process, a chemical reaction occurs in which a hydrogen coating is formed on silica with hydroxyl groups in the silanol group (SiOH). The chemical reaction of silica silanization is expressed in Eq. (1) as follows (Hayichelaeh *et al*. 2018).

$$\equiv S_i\text{—}OH_{:\,Solid} + C_8H_{17}Si(OC_2H_5)_{3:\,Liquid} \Rightarrow \equiv S_i\text{—}O\text{—}Si(OC_2H_5)_2C_8H_{17:\,Solid} + C_2H_5OH_{:\,Liquid} \quad (1)$$

After this process, the soil sample treated chemically with two hydrophobizing polymers was put into a drying oven (110–120°C) for 24 hours to complete the hydrophobization treatment.

3.3 Test conditions for each case

3.3.1 Case 1: Effect of rainfall intensity

Rainfall infiltration occurs on embankment slopes under various rainfall conditions and is the main cause of slope failure. Slope failure is internally related to the type of ground layer soil and the mechanical and hydraulic properties according to various conditions, but external influences such as rainfall intensity and duration also have a great influence. In Case 1 of the laboratory embankment model test of this study, the water-shielding performance of the hydrophobic material layer was examined under three rainfall conditions: I= 20 mm/h for Case 1-1, I= 100 mm/h for Case 1-2, and I= 100 mm/h for Case 1-3. Here, three rainfall intensities of 20, 50, and 100 mm/h were set to represent extreme rainfall conditions, heavy rainfall such as showers, and general rainfall, respectively (Mirhosseini *et al*. 2013). The applicability of the impermeable layer of hydrophobic material to water infiltrating into the slope was investigated through these three rainfall intensities. On the other hand, according to the results of the WIH test by Kim *et al*. (2021), the hydrophobic Toyoura sand, which has the smallest mean particle size ($D_{50\text{-}min}$), showed sufficient water impermeability as WIH value= 14.2 cm under a dry density of ρ_d=1.50 g/cm^3. For comparison with the WIH test, in Case 1, the hydrophobic layer using Toyoura sand was prepared with the same dry density.

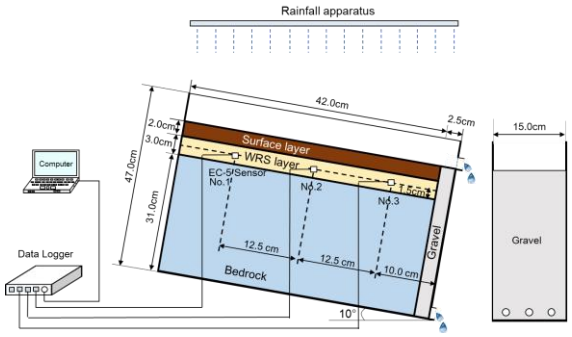

Fig. 7 Schematic diagram of model test for Case 1

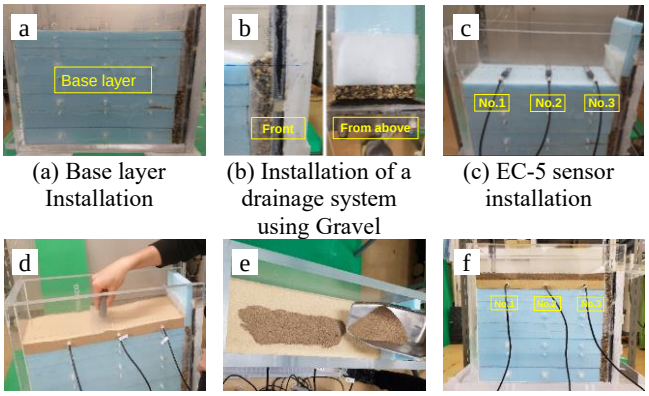

(a) Base layer Installation (b) Installation of a drainage system using Gravel (c) EC-5 sensor installation

(d) Hydrophobic layer installation (e) Surface layer installation (f) Installation complete

Fig. 8 Production process of model test for Case 1

Table 2 Test conditions for Case 1

Case No.		1-1	1-2	1-3
Thickness of surface layer (cm)		2.0	2.0	2.0
Thickness of hydrophobic layer (cm)		3.0	3.0	3.0
Initial dry density, ρ_{di} (g/cm^3)	Surface layer	1.50	1.50	1.50
	Hydrophobic layer	1.50	1.50	1.50
	Drainage path (gravel)	1.64	1.64	1.64
Rainfall intensity, *I* (mm/hr)		20	50	100
Slope angle, Φ (°)		10	10	10
Measurement time, *t* (h)		5	5	5

As shown in Fig. 7, a model embankment for Case 1 was comprised of a surface hydrophilic Masado layer of 2.0 cm under a dry density of ρ_d=1.50 g/cm^3 and the hydrophobic Toyoura sand layer (i.e., water repellent sand (WRS) layer) of 3.0 cm under a dry density of ρ_d=1.50 g/cm^3. EC-5 sensors were also installed in three places in the hydrophobic layer to evaluate rainfall infiltration behavior. Fig. 8 shows the production process of the model test for Case 1. A drainage system using Gravel was prepared under a dry density of ρ_d=1.64 g/cm^3. The slope

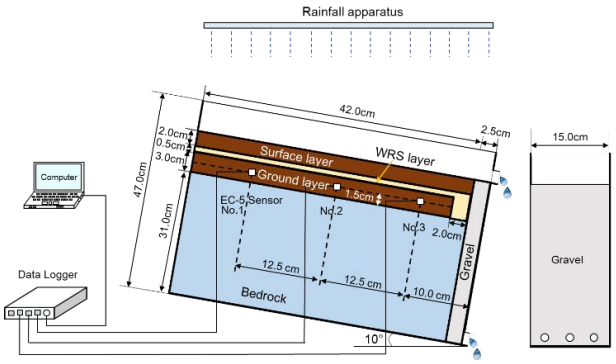

Fig. 9 Schematic diagram of model test for Case 2

Table 3 Test conditions for Cases 2 & 3

Case		No. 2	No. 3
Thickness of surface layer (cm)		2.0	2.0
Thickness of hydrophobic layer (cm)		0.5	3.0
Thickness of Masado layer (cm)		3.0	3.0
Initial dry density, ρ_{di} (g/cm^3)	Surface layer	1.50	1.50
	Hydrophobic layer	1.50	1.50
	Lower layer	1.50	1.50
	Drainage path (gravel)	1.64	1.64
Rainfall intensity, *I* (mm/hr)		100	100
Slope angle, Φ (°)		10	10
Measurement time, *t* (h)		5	5

angle (Φ) is 10°. The model test was conducted for 5 hours. Table 2 summarizes the test conditions for Case 1.

3.3.2 Case 2: Effect of layer thickness

When installing hydrophobic geomaterial on a slope, the amount of soil used is determined by the layer thickness. Since the layer thickness is related to the construction cost, the thinner the layer, the higher the economic efficiency is evaluated. Thus, in Case 2, the water-shielding performance of a thin layer of hydrophobic material was investigated. As shown in Fig. 9, a model embankment was prepared consisting of a lower hydrophilic layer of 3.0 cm equipped with EC-5 sensors to determine rainfall infiltration, a middle hydrophobic Toyoura sand (i.e., WRS) layer of 0.5 cm, and a 2.0 cm surface hydrophilic layer. In addition, to prevent water from infiltrating through the drainage path using Gravel on the right side of the model, a hydrophobic material (i.e., hydrophobic Toyoura sand) was placed with a thickness of 2.0 cm on the right side of the bottom layer.

According to the WIH test results of Kim *et al*. (2021), the results of the WIH test showed that all hydrophobic Silica sands with a mean particle size of 2.90 mm or more (i.e., Silica sand No. 2) have water-shielding performance if the layer thickness is greater than 0.45 cm. Here, the WIH value of Silica sand No. 2 is 1.0 cm. In particular, the hydrophobic Toyoura sand, which has the smallest mean grain size, showed sufficient water-shielding performance (i.e., WIH=14.2 cm) if the layer thickness is greater than 0.15 cm. Thus, in Case 2, the middle layer of the

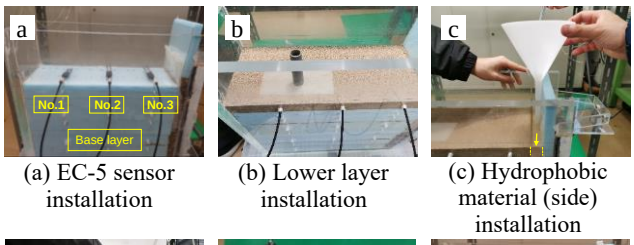

(a) EC-5 sensor installation (b) Lower layer installation (c) Hydrophobic material (side) installation

(d) Hydrophobic layer installation (e) Surface layer installation (f) Installation complete

Fig. 10 Production process of model test for Case 2

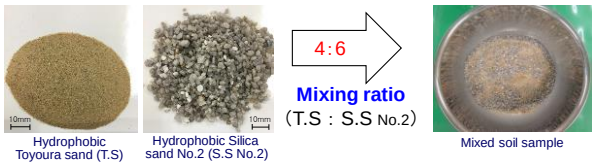

Fig. 11 Sample mixed with hydrophobic Toyoura sand and Silica sand No.2 in a ratio of 4:6 in Case 3

hydrophobic Toyoura sand was prepared with the thinnest thickness of 0.5 cm that can be efficiently produced in the laboratory model test under ρ_d=1.50 g/cm^3. The rainfall intensity condition is I= 100 mm/h, and the slope angle (Φ) is 10°. The model test was conducted for 5 hours. Table 3 summarizes the test conditions of Case 2. Fig. 10 shows the production process of a model test for Case 2. A drainage system using Gravel was prepared under a dry density of ρ_d=1.64 g/cm^3.

3.3.3 Case 3: Effect of grain size distribution of geomaterials

Although various sandy soils can be used as hydrophobic geomaterials, their grain size distributions are different. Since the water-shielding performance of hydrophobic materials is affected by the size of the soil particles, it is necessary to examine the water-shielding performance of the hydrophobic layer with respect to the change in particle size distribution.

According to the WIH test results of Kim *et al*. (2021), it was reported that the water-shielding performance (WIH = 11.9 cm) was excellent when the content of soil particles smaller than 2.0 mm was 40% or more using a mixed sample of hydrophobic Toyoura sand and hydrophobic Silica sand No. 2. Thus, in Case 3, the effect of grain size distribution on the water-shielding performance of the hydrophobic layer was examined using a mixed hydrophobic material with a mixing ratio (Toyoura sand: silica sand No. 2) of 4:6 as shown in Fig. 11. Fig. 12 shows the grain size distribution curves of Toyoura sand, Silica sand No.2, and a mixed sample with a mixing ratio of 4:6 in Case 3. As shown in Fig. 13, a model embankment was created with a surface layer of 2.0 cm, a mixed hydrophobic material layer of 3.0 cm, and a lower layer of 3.0 cm for

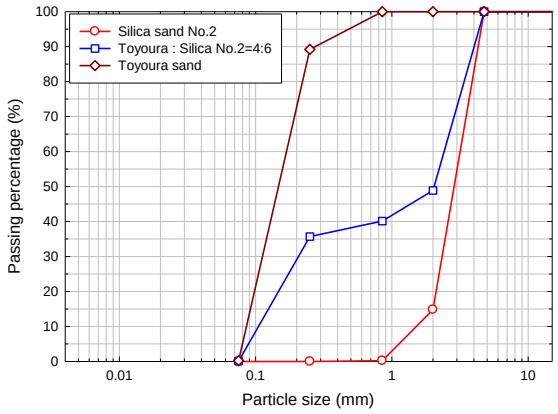

Fig. 12 Grain size distribution curves of Toyoura sand, Silica sand No.2, and a mixed sample with a mixing ratio of 4:6 in Case 3

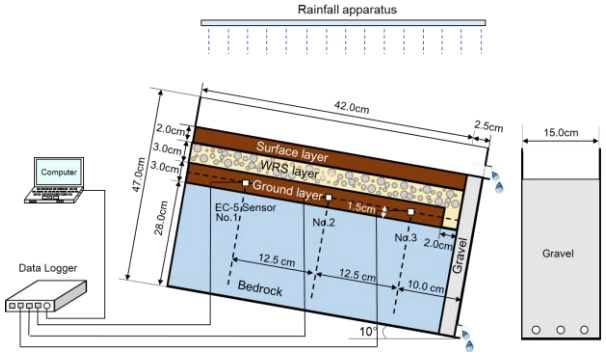

Fig. 13 Schematic diagram of model test for Case 3

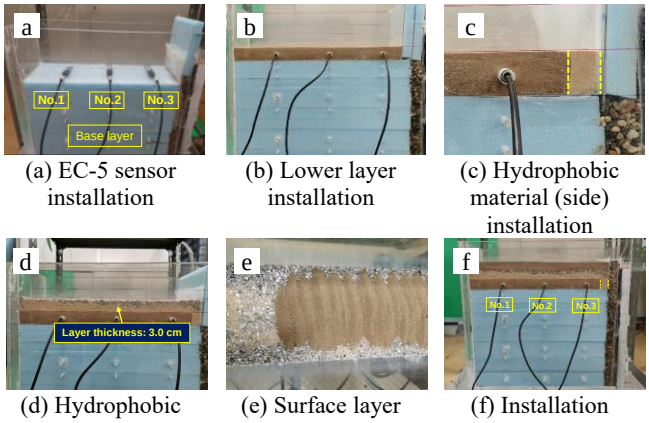

(a) EC-5 sensor installation (b) Lower layer installation (c) Hydrophobic material (side) installation

(d) Hydrophobic layer installation (e) Surface layer installation (f) Installation complete

Fig. 14 Production process of model test for Case 3

installing the EC-5 sensor. As in Case 2, hydrophobic Toyoura sand was installed on the side to prevent water from infiltrating the drainage path. To measure the rainfall infiltration, a lower layer was installed with three EC-5 sensors under the mixed hydrophobic material layer. The rainfall intensity condition is I= 100 mm/h, and the slope angle (Φ) is 10°. The model test was conducted for 5 hours. The test condition for Case 3 is summarized in Table 3. Fig. 14 shows the production process of the model test for Case 3. A drainage system using Gravel was prepared under a dry density of ρ_d=1.64 g/cm^3.

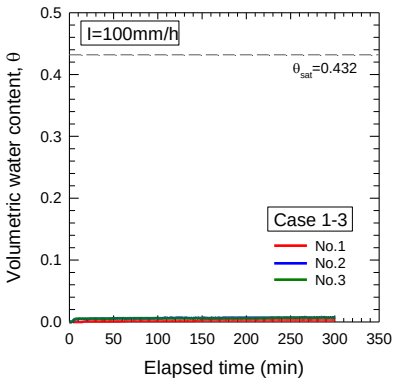

Fig. 15 Results measured by the EC-5 sensors for Case 1-3: The saturated volumetric moisture content (θ_{sat}) of the 2-cm-thick WRS layer was 0.432, but there was little change (due to noise) in the volumetric water content because no rainfall infiltration occurred during the 5-hour test

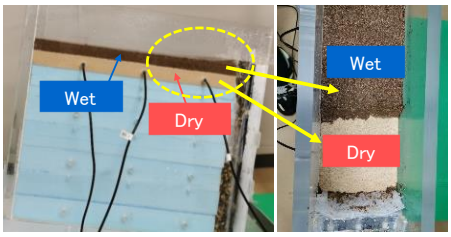

Fig. 16 Internal condition after removal of the surface layer for Case 1

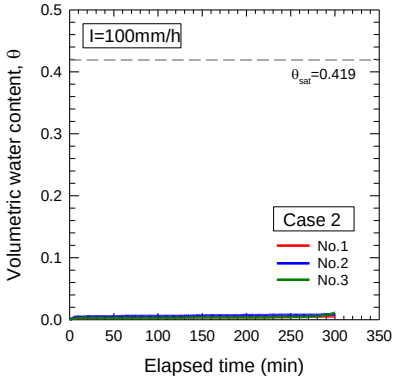

Fig. 17 Results measured by the EC-5 sensors for Case 2: Under the condition of the presence of a ground layer (θ_{sat} = 0.419) beneath the 5-mm thick WRS layer, there was little change (due to noise) in the volumetric water content because no rainfall infiltration occurred during the 5-hour test

3.4 Test results of each case

3.4.1 Result of Case 1: Effect of rainfall intensity

Fig. 15 shows the result measured by the EC-5 sensors for I= 100 mm/h for Case 1-3, the strongest rainfall condition. Measurements were performed for 5 hours at rainfall intensities of 20 mm/h, 50 mm/h, and 100 mm/h. As shown in Fig. 15, no response was observed from the EC-5 sensors at any rainfall intensity after the measurement was completed. Although subtle changes due to noise were

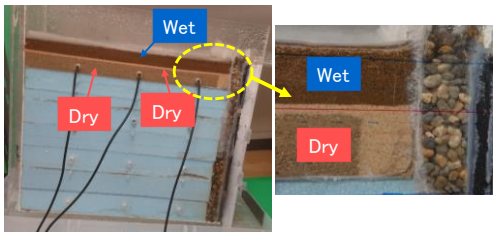

Fig. 18 Internal condition after removal of the surface layer for Case 2

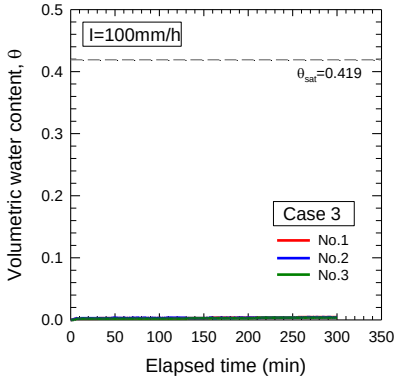

Fig. 19 Results measured by the EC-5 sensors for Case 3: Under the condition of having a ground layer (θ_{sat} = 0.419) below the mixed soil WRS layer, there was little change (due to noise) in the volumetric water content because no rainfall infiltration occurred during the 5-hour test

detected during the measurements, there is no response to rainfall infiltration. Because the saturated volumetric water content (θ_{sat}) of the WRS layer is 0.432, these subtle changes can be ignored. On the other hand, water infiltrates into the surface layer immediately after the start of the experiment, and the surface layer was completely wet when the experiment was finished as shown in Fig. 16. Meanwhile, the hydrophobic layer underneath was dry for 5 hours. From these results, it was found that rainwater did not infiltrate into the hydrophobic layer even under the extreme condition of a rainfall intensity of 100 mm/h, and the excellent water-shielding performance of the hydrophobic layer could be demonstrated in Case 1.

3.4.2 Result of Case 2: Effect of layer thickness

Fig. 17 shows the results measured by the EC-5 sensors for Case 2. After 5 hours of measurement with a rainfall intensity of 100 mm/h, no response was observed from the sensors (Nos. 1, 2, and 3) for testing. Here, the saturated volumetric water content (θ_{sat}) of the lower layer is 0.419. Water infiltrated into the surface hydrophilic layer immediately after the experiment started, and the surface hydrophilic layer was completely wet after the experiment ended as shown in Fig. 18. While the hydrophobic Toyoura sand and the lower hydrophilic layers were dry. It was found from this result that even if a very thin hydrophobic layer of 0.5 cm (ρ_d= 1.50 g/cm^3) is formed, rainwater does not infiltrate under the hydrophobic layer, maintaining excellent water-shielding performance. It is expected that the construction costs for hydrophobic geomaterials could

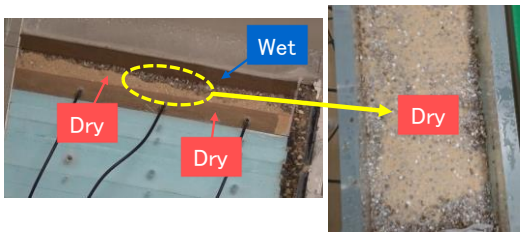

Fig. 20 Internal condition after removal of the surface layer for Case 3

be reduced by decreasing the thickness of the hydrophobic layer when applied to engineered slopes.

3.4.3 Result of Case 3: Effect of grain size distribution of geomaterials

The results of the volumetric water content measured by the EC-5 sensor are shown in Fig. 19. The measurement was made for 5 hours with a rainfall intensity of 100 mm/hr, but no response was observed from the EC-5 sensors (Nos. 1, 2, & 3) until the endpoint. As in Cases 1 & 2, some fluctuations are also detected in Case 3. Since the saturated volumetric water content (θ_{sat}) of the lower layer is 0.419, it can be understood that this is due to noise during measurement. Water infiltrated the surface layer immediately after the experiment began, and after the experiment ended, the surface layer was wet as shown in Fig. 20.

On the other hand, the soil layer where the sensors were installed and the hydrophobic material on the side were dry. The mixed hydrophobic material layer showed some infiltration in the hydrophobic Silica sand No. 2 section, but no infiltration in the hydrophobic Toyoura sand section. Thus, it was found that water does not infiltrate beneath the mixed hydrophobic layer and that it is exerting a water-shielding performance. Moreover, from the results of the sample mixed with hydrophobic Toyoura sand and Silica sand No.2 in a ratio of 4:6, it can be determined whether the water-shielding performance is achieved based on a content ratio of soil particles of 2.0 mm or less at the actual construction site. Therefore, it can be understood that if the content ratio of soil particles of 2.0 mm or less is 40% or more, the hydrophobic layer exhibits water-shielding performance when applied to engineered slopes.

4. Case-specific review and implications

In this study, the applicability of hydrophobic materials to impermeable layers was examined through laboratory embankment model tests for three cases. In Case 1, the impermeable layer of hydrophobic materials did not allow rain infiltration even under the extreme condition of 100 mm/h rainfall intensity. Thus, it can be said that it can be used as an impermeable layer material for rain infiltration. On the other hand, from the results of Case 2, it was found that rain infiltration did not occur even under the extreme condition of I= 100 mm/h for an impermeable layer thickness of 5 mm. From this result, it is judged that it is possible to construct an impermeable layer thickness of 5

mm or more for an actual engineering slope. However, since it is more difficult to construct an actual slope with a layer thickness of 5 mm as in this study, it would be better to design a layer thickness thicker than this for on-site constructability.

Finally, from the results of Case 3, the water-shielding performance of the mixed hydrophobic materials was confirmed. In particular, since the water-shielding performance of mixed hydrophobic materials is not affected by the fine-grained content, a hydrophobic ground material with a higher fine-grained content would be able to be made. However, since the shear strength generally decreases as the fine-grained content increases, additional shear strength tests for mixed hydrophobic materials should be conducted for application to engineering slopes. The experimental results using Toyoura sand and silica sand in this study can be used as a reference for the applicability to actual field slopes and the selection of hydrophobic materials. Unfortunately, however, there are still few useful research results on hydrophobic materials in the field of geotechnical engineering. Therefore, additional experiments on hydrophobic materials should be conducted because many ground materials can be hydrophobic materials and the range of choices is wide.

5. Conclusions

In this study, to evaluate the water-shielding performance of hydrophobic geomaterials and their applicability at actual engineered slopes, a series of laboratory embankment model tests based on the WIH test results of Kim *et al*. (2021) was performed on three effects: (1) Case 1: Rainfall intensity, (2) Case 2: Effect of layer thickness, (3) Case 3: Effect of grain size distribution of geomaterials. From the results of this study, the following conclusions are drawn.

(1) In Case 1, the laboratory embankment model tests were conducted under three rainfall intensity patterns (i.e., 20 mm/h, 50 mm/h, and 100 mm/h). As a result, rainwater did not infiltrate into the hydrophobic layer at any rainfall intensity, and the excellent water-shielding performance of the hydrophobic layer was revealed. Thus, it was found that the installation of a hydrophobic layer is effective as a measure against slope collapse due to rain infiltration.

(2) In Case 2 for the effect of layer thickness, the very thin hydrophobic layer of 0.5 cm under the rainfall intensity of 100 mm/h for 5 hours was applied. Since rainwater did not infiltrate below the hydrophobic layer, it was found that excellent water-shielding performance was maintained. Thus, it is expected that the construction costs could be reduced by decreasing the thickness of the hydrophobic layer.

(3) In Case 3 for the effect of the grain size distribution of hydrophobic geomaterials, a mixed hydrophobic material with a mixing ratio (Toyoura sand: Silica sand No. 2) of 4:6 was used. No rainwater infiltration occurred downward in the mixed hydrophobic material layer. Thus, if hydrophobic materials involved the content ratio of soil particles of 2.0 mm or less is over 40%, the hydrophobic layer could exhibit water-shielding performance when applied to engineered slopes.

Acknowledgments

This work was supported by the National Research Foundation of Korea (NRF) grant funded by the Korea government (MSIT) (No. RS-2023-00221184).

References

Bauters, T.W.J., Steenhuis, T.S., DiCarlo, D.A., Nieber, J.L., Dekker, L.W., Ritsema, C.J., Parlange, J.Y. and Haverkamp, R. (2000), "Physics of water repellent soils", *J. Hydrol*., **231**, 233-243. https://doi.org/10.1016/S0022-1694(00)00197-9.

Debano, L.F. and Krammes, J.S. (1966), Water repellent soils and their relation to wildfire temperatures", *Hydrolo. Sci. J*., **11**(2), 14-19. https://doi.org/10.1080/02626666609493457.

Doerr, S.H., Shakesby, R.A., Dekker, L.W. and Ritsema, C.J. (2006), "Occurrence, prediction and hydrological effects of water repellency amongst major soil and land-use types in a humid temperate climate", *Eur. J. Soil Sci.*, **57**(5), 741-754. https://doi.org/10.1111/j.1365-2389.2006.00818.x.

Doan, N.S. (2023), "Reliability analysis and uncertainty quantification of clay and sand slopes stability evaluated by Fellenius and Bishop's simplified methods", *Int. J. Geo-Eng.*, **14**(1), 22. https://doi.org/10.1186/s40703-023-00200-2.

Feng, G.L., Letey, J. and Wu, L. (2001), "Water ponding depths affect temporal infiltration rates in a water-repellent sand", *Soil Sci. Soc. Am. J.*, **65**(2), 315-320. https://doi.org/10.2136/sssaj2001.652315x.

Fredlund, D.G., Morgenstern, N.R. and Widger, R.A. (1978), "The shear strength of unsaturated soils", *Can. Geotech. J.*, **15**(3), 313-321. https://doi.org/10.1139/t78-029.

Hayichelaeh, C., Reuvekamp, L.A.E.M., Dierkes, W.K., Blume, A., Noordermeer, J.W.M. and Sa-hakaro, K. (2018), "Enhancing the silanization reaction of the silica-Silane system by different amines in model and practical silica-filled natural rubber compounds", *Polymers*, **10**(6), 584. https://doi.org/10.3390/polym10060584.

Heibaum, M. (2016), *Geotextiles used in filtration*, In Geotextiles 257-275. Woodhead Publishing. https://doi.org/10.1016/B978-0-08-100221-6.00012-7.

Jaramillo, D.F., Dekker, L.W., Ritsema, C.J. and Hendrickx, J.M.H. (2000), "Occurrence of soil water repellency in arid and humid climates", *J. Hydrol*., **231**, 105-111. https://doi.org/10.1016/S0022-1694(00)00187-6.

Karube, D. and Kawai, K. (2001), "The role of pore water in the mechanical behavior of unsaturated soils", *Geotech. Geol. Eng.*, **19**, 211-241. https://doi.org/10.1023/A:1013188200053.

Kim, B.S., Shibuya, S., Park, S.W. and Kato, S. (2010), "Application of suction stress for estimating unsaturated shear strength of soils using direct shear testing under low confining pressure", *Can. Geotech. J*., **47**(9), 955-970. https://doi.org/10.1139/T10-007.

Kim, B.S., Ren, D., Park, S.W. and Kato, S. (2021), "Establishing selection criteria of water repellent sandy soils for use in impervious layer of engineered slope", *Constr. Build. Mater.*, **293**, 123551. https://doi.org/10.1016/j.conbuildmat.2021.123551.

Lee, M., Chang, I., Kang, S.J., Lee, D.H. and Cho, G.C. (2023),

"Alkaline induced-cation crosslinking biopolymer soil treatment and field implementation for slope surface protection", *Geomech. Eng*, **33**(1), 29-40. https://doi.org/10.12989/gae.2023.33.1.029.

Li, A., Liu, Y. and Szlufarska, I. (2014), "Effects of interfacial bonding on friction and wear at silica/silica interfaces", *Tribology Lett.*, **56**(3), 481-490. https://doi.org/10.1007/s11249-014-0425-x.

Meek, A.H., Beckett, C.T. and Elchalakani, M. (2020), "Alternative stabilised rammed earth materials incorporating recycled waste and industrial by-products: Durability with and without water repellent", *Constr. Build. Mater.*, **265**, 120629. https://doi.org/10.1016/j.conbuildmat.2020.120629.

Mirhosseini, G., Srivastava, P. and Stefanova, L. (2013), "The impact of climate change on rainfall Intensity–Duration–Frequency (IDF) curves in Alabama", *Reg. Environ. Change*, **13**, 25-33. https://doi.org/10.1007/s10113-012-0375-5.

Oh, W.T. and Vanapalli, S. (2018), "Undrained shear strength of unsaturated soils under zero or low confining pressures in the vadose zone", *Vadose Zone J.*, **17**(1), 1-13. https://doi.org/10.2136/vzj2018.01.0024.

Rahardjo, H., Ong, T.H., Rezaur, R.B. and Leong, E.C. (2007), "Factors controlling instability of homogeneous soil slopes under rainfall", *J. Geotech. Geoenviron. Eng*., **133**(12), 1532-1543. https://doi.org/10.1061/(ASCE)1090-0241(2007)133:12(1532)

Rajabian, A. (2023), "Effect of initial failure geometry on the progress of a retrogressive seepage-induced landslide", *Int. J. Geo-Eng.*, **14**(1), 11. https://doi.org/10.1186/s40703-023-00189-8.

Ritsema, C.J., Dekker, L.W., Nieber, J.L. and Steenhuis, T.S. (1998), "Modeling and field evidence of finger formation and finger recurrence in a water repellent sandy soil", *J. Water Resour. Res.*, **34**(4), 555-567. https://doi.org/10.1029/97WR02407.

Ritsema, C.J. and Dekker, L.W. (2000), "Preferential flow in water repellent sandy soils: principles and modeling implicationsv", *J. Hydrol.*, **231**, 308-319. https://doi.org/10.1016/S0022-1694(00)00203-1.

Sun, D.A., Sheng, D., Xiang, L. and Sloan, S.W. (2008), "Elastoplastic prediction of hydro-mechanical behaviour of unsaturated soils under undrained conditions", *Comput. Geotech.*, **35**(6), 845-852. https://doi.org/10.1016/j.compgeo.2008.08.002.

Vigil, G., Xu, Z., Steinberg, S. and Israelachvili, J. (1994), "Interactions of silica surfaces", *J. Colloid Interface Sci.*, **165**(2), 367-385. https://doi:10.1006/jcis.1994.1242.

Wallis, M.G. and Horne, D.J. (1992), "Soil water repellency", *Adv. Soil Sci.*, **20**, 91-146. https://doi.org/10.1007/978-1-4612-2930-8_2.

Yu, J.Y., Woo, J.W., Kang, K.N. and Song, K.I. (2023), "Correlations between variables related to slope during rainfall and factor of safety and displacement by coupling analysis", *Geomech. Eng.*, **33**(1), 77-89. https://doi.org/10.12989/gae.2023.33.1.077.